



Article

Modeling, Simulation, and Computer Control of a High-Frequency Wood Drying System

Predrag Stolic ^{1,*} , Zoran Stevic ^{1,2}, Sanja Petronic ³, Vojkan Nikolic ⁴, Misa Stevic ⁵, Dragan Kreculj ⁶ 
and Danijela Milosevic ⁷

¹ Technical Faculty in Bor, University of Belgrade, VJ 12, 19210 Bor, Serbia

² School of Electrical Engineering, University of Belgrade, Bulevar kralja Aleksandra 73, 11120 Belgrade, Serbia

³ Institute of General and Physical Chemistry, Studentski trg 12/V, 11158 Belgrade, Serbia

⁴ Department of Information Technology, University of Criminal Investigation and Police Studies, Cara Dusana 196, 11080 Belgrade, Serbia

⁵ Elsys Eastern Europe, Omladinskih brigada 90e, Airport City, Building 2300, 11070 Belgrade, Serbia

⁶ Department of Electrical and Computer Engineering, The Academy of Applied Technical Studies, Katarine Ambrozic 3, 11000 Belgrade, Serbia

⁷ Faculty of Technical Sciences, University of Kragujevac, Svetog Save 65, 32102 Cacak, Serbia

* Correspondence: pstolic@tfbor.bg.ac.rs

Abstract: High-frequency wood drying is the modern method used in raw wood drying so that treated wood can be used further in various processes. Such systems are used because of the economy, energy efficiency, obtaining of good mechanical properties of the wood after treatment, as well as reducing time consumption. Therefore, it is extremely important to understand each component of such systems and processes. The mentioned systems are implemented using high-frequency generators based on vacuum tubes (VT). Their development and, in particular, optimization are by far more complex than the transistor systems; therefore, the development is now compelled to rely on computer modelling and simulation. In this research, a high-frequency (HF) generator of 20 kW output power and 1.5–15 MHz adjustable frequency based on VT was produced and then, with the corresponding model for VT itself and the rest of the developed circuit, was followed by computer simulation and real-system measurement. The model parameters were adjusted, which provided additional system optimization. An extra match of the results from the simulation and measurement was obtained; thus, the optimization was performed faster and more precisely. In addition, an easier and quicker way of adjusting parameters of the PID controller using a developed software-based control system was attained. The problems of cooling the VT anode under high DC voltage, as well as temperature measurement in the HF electric field, have been solved.

Keywords: control; generator; modeling; simulation; wood industry



Citation: Stolic, P.; Stevic, Z.; Petronic, S.; Nikolic, V.; Stevic, M.; Kreculj, D.; Milosevic, D. Modeling, Simulation, and Computer Control of a High-Frequency Wood Drying System. *Electronics* **2023**, *12*, 226. <https://doi.org/10.3390/electronics12010226>

Academic Editor: Haibo Shu

Received: 11 December 2022

Revised: 24 December 2022

Accepted: 30 December 2022

Published: 2 January 2023



Copyright: © 2023 by the authors. Licensee MDPI, Basel, Switzerland. This article is an open access article distributed under the terms and conditions of the Creative Commons Attribution (CC BY) license (<https://creativecommons.org/licenses/by/4.0/>).

1. Introduction

The use of wood as a material still achieves a significant market share today. Wood is used in different segments of production, whether it is the production of wood for further use, as building materials (wooden boards, beams, plates etc.), and in the production of parquet, furniture, entire houses, or the production of firewood. However, raw wood cannot be directly used in production since it always has the appropriate amount of moisture in it and, accordingly, its application is largely limited. In order to achieve a wider application of wood, the aforementioned moisture must be removed; that is, in further application, the wood must be treated with some drying treatment. Wood after the drying treatment manifests better properties in terms of strength, rotting, and retention of dimensions after processing.

In general, there are several different methods of drying, and, therefore, different approaches when the narrowed area of wood drying is discussed [1]. Certainly one of

the oldest principles of wood drying is natural drying; however, this type of drying is largely limited by the quality of drying itself, by a number of natural factors, as well as the time required to achieve the appropriate drying results. In accordance with that, the industry has been looking for different principles of drying that would improve wood drying technology itself on several grounds, starting with the primary improvements to achieve a better percentage of wood drying, that is, a lower percentage of the presence of moisture, better mechanical properties of the dried wood itself, minimized time needed to achieve the appropriate drying results, increased energy efficiency, and cost reduction [2,3]. Technical and technological progress in various spheres of science and technology leads, among other things, to significant improvements in the field of wood drying.

Chamber drying methods are one of the most common types of wood drying, so for a while, the primary focus in research has been the improvement of the chamber in which drying is carried out and better characterization of the processes that are realized using convective drying [4]. Although numerous improvements have been achieved in this segment of work, it must be noted that theoretical and empirical results indicate that this approach to wood drying has reached its maximum potential. That is why there are new approaches in the implementation of wood drying that enable further improvement of the end product in terms of its quality, but also further improvement of the processes by which the drying is realized.

One such approach is the approach based on the use of a High-Frequency Current (HFC) and the so-called high-frequency current drying (HFC drying), which became feasible thanks to the progress made in the production of industrial high-frequency (HF) generators stemming from decades of progress in electronics and high technologies based on it. It should be noted here that HFC drying can be realized independently, or it can be combined with convection, and high-frequency (dielectric) heating can be used in various types of industry (furniture, textile, paper, and other industries) [5]. When the application in the field of wood drying is mentioned, the basis of the HFC wood drying system is a high-frequency AC generator. Because of the use of high voltage and the realization of large powers, electronic tubes are in use in most cases, as they provide adequate efficiency, although there are versions in which the use of modern powerful transistors is also possible, but it is limited to smaller installations such as laboratory ones [6–11]. Following modern trends, as with most systems today, measurement and control, that is automatic regulation, is achieved using specialized software solutions [12]. Appropriate software enables accuracy, timeliness, and a better mastering of the complexity of the system from the end user point of view. In some versions of the system, Adaptive Fuzzy Controllers (AFC) are also used, which in their work use various methods based on various variations of gradient-descent methods, the least square method, linear and non-linear regression, the linguistically based rule extraction, and others [13–16]. In order to better understand the process itself and carry out its adequate parameterization, optimization and further improvement, the most modern systems today use tools from the domain of data science and artificial intelligence, such as Artificial Neural Networks (ANN), Machine Learning (ML), etc. Very large and complex plants are based on SCADA systems so that the entire process can be adequately monitored [17].

As can be seen from the above, it can be said that today's modern HFC wood drying systems are consisted of two main units. The first unit represents a traditional HFC wood drying system and the second one represents the accompanying hardware-software component.

Different approaches to wood drying have been based on the use of fossil fuels for a long time. In many cases, those approaches are still used today. However, the use of fossil fuels for these purposes has become questionable from the various issues' point of view. There were problems with supply chains, as well as with the creation of more significant direct and indirect costs, and it should be noted that, from an ecological point of view, a very significant negative impact on the environment is manifested. In accordance with that, the wood industry has switched to methods based on the use of electricity instead of fossil fuels. Today, the most common approaches are based on the use of radio

frequencies. However, the use of radio frequencies also has certain limitations during use and there can be a certain increase in operating costs when we compare the use of electricity and fossil fuels in the same domain. The use of high frequencies contributes to overcoming certain limitations manifested by the use of radio frequencies; however, their design and development is more complex and may produce additional economic efforts. In this sense, a significant reduction can be achieved by proper modeling and appropriate optimizations. By introducing appropriate simulation methods and approaches, as well as adequate computer control, the use of high frequencies can bring a number of benefits when implementing such systems for removing moisture from wood.

In accordance with this, in this paper, a model of a semi-industrial high-frequency drying system is proposed, as well as the computer simulation and experimental confirmation. Furthermore, automatic temperature control of wood based on the developed adequate software solution is shown.

2. Construction of HF High Power Generator

High-frequency wood dryers use only electricity for drying and, compared with traditional kiln dryers, they are more efficient because they significantly reduce the required time for realization of the drying process. The use of high-frequency heating in wood treatment is appropriate because wood is a non-conducting material, so dielectric heating is applicable in this case and consistent heating of material can also be achieved. This type of heating is accomplished using an alternating electromagnetic field of varying frequencies [18,19]. As mentioned before, one of the crucial elements in the construction of these wood dryers is the high-frequency generator.

In the area of lower and middle frequencies, transistor generators are predominant. However, in the case of radio frequencies (1 MHz and higher), transistor generators have very limited possibilities. With larger powers (tens of kW and more), the advantage is on the side of the generator with vacuum tubes (VT). More precisely, these requirements are placed in front of the wood drying generators, and they are still most often based on VT [14–16,20].

The basis of the presented high-frequency (HF) generator is a Colpitts oscillator whose principle scheme is shown in Figure 1. The VT triode GU62A is used as an active element (AE). Passive elements of the oscillator circuit are capacitors C_1 and C_2 and inductor L_2 . At the same time, the capacitance C_2 includes the capacitance of the consumer, which also has a parallel resistance R_L .

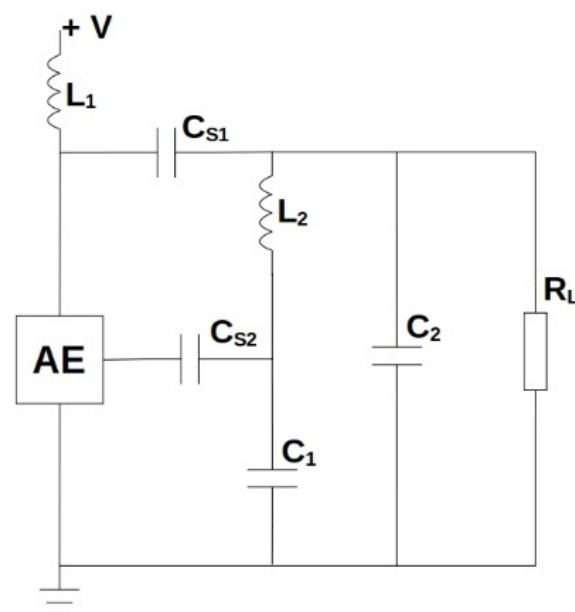


Figure 1. Principal scheme of the Colpitts oscillator.

The high-capacity capacitor C_{S1} blocks the penetration of the DC power supply to the oscillator circuit and the consumer, and the positive feedback is achieved by the capacitor C_{S2} . The inductor L_1 of high inductance prevents penetration of HF oscillations towards the DC source.

The inductance L_2 and the equivalent capacitance C of series-connected capacitors C_1 and C_2 determine the frequency of oscillation:

$$f = \frac{1}{2\pi\sqrt{CL_2}}$$

Depending on the type of wood being dried, as well as the moisture content, the oscillation frequency is adjusted from 1.5 to 15 MHz [5,21–23].

Applying the procedures given in [6,21–26], the other parameters of the HF generator are calculated and the details will be given for a specific designed generator with a power of 20 kW intended for drying 4 m³ of wood as it shown in Table 1.

Table 1. Input parameters for generator calculation [20].

Variable	Value
Nominal output power	$P = 20$ kW
Anode DC voltage	$V_a = 4$ kV
Braking voltage	$E_g' = -200$ V
Nominal anode dissipation	$P_a = 40$ kW
Nominal grid dissipation	$P_g = 1.8$ kW
Gradient of characteristics	$S = 45$ mA/V
Amplification	$\mu = 19$

Calculation of the parameters of the regime [23–26]:

The cut-off angle (adopted according to the recommendation [25]): $\theta = 85^\circ$. Based on the range of the recommended values for the given VT and the selected cut off angle, the coefficients are determined as follows: $\alpha_1 = 0.488$, $\beta = 0.446$, $\gamma = 1.611$, and $\xi = 0.85$.

Based on the obtained coefficients, the electrical parameters are calculated:

Maximum anode voltage:

$$U_{ma} = \xi V_a = 3200 \text{ V}$$

Anodic current pulse:

$$I_{a1} = \frac{2P}{U_{ma}} = 12.5 \text{ A}$$

DC component of anode current:

$$I_{a0} = \frac{I_{a1}}{\gamma} = 7.76 \text{ A}$$

Power consumption:

$$P_0 = I_{a0} V_a = 31 \text{ kW}$$

Anodic dissipation power:

$$P_a = P_0 - P = 11 \text{ kW}$$

The obtained anode dissipation power is far less than the permitted one (40 kW), which means that the calculation of the energy part of the circuit is satisfactory, but also that there is a large reserve of power. It is similar to the grid dissipation power (calculated $P_g = 1.11$ kW, which is significantly lower than the limit value (1.8 kW)).

Since the VT anode is under a high DC voltage and water cooling is necessary (dissipation power is high), a special system with water recirculation through long hoses

was created, which ensures a sufficient flow of water, and also a sufficient high electrical resistance towards grounded ends in order to get the leakage current below 1 mA.

By applying the procedures and recommendations from [6,25], the parameters of the passive elements were calculated and shown in Table 2.

Table 2. Passive elements for generator [20].

Variable	Value
C_1	6.5 nF
C_2	5 nF
C_{S1}	160 nF
C_{S2}	250 nF
L_1	30 mH
L_2	2.5 μ H

3. Modeling of the HF Generator

The typical amplifier stage of the oscillator functions as a voltage-controlled current source. This means that the input voltage minimizes the output load of the parallel LC network, whereas the current output minimizes the input load of the LC circuit. The example of such a device is an active device with a vacuum tube, as is the case in these circumstances. In simulations, the amplifier circuit can be replaced by an ideal source of controlled voltage (VCCS) with an advanced transconductance G_m . The use of VCCS is not necessary, but it makes it easier to interpret the transfer function from input to output voltage. Moreover, the VCCS allows the floating nodes to be supplied from the common test signal when necessary.

PSpice simulation software embedded in the OrCAD package [27] was used to simulate the behavior of the projected HF generator. The basic scheme of the generator from Figure 1 was supplemented by serial inductances (L_3 to L_8) that correspond to the real inductances of the lines. Also included in the system was the resistor R_1 that corresponded to the active consumption, that is, the drying of the wood. The transient analysis was performed, but DC parameters were checked.

The starting model for the active element-triode was SV811-3 [28–30]. The basic parameters of the model were calculated according to the recorded static characteristics of VT, whereas the parasitic capacitances were taken from the manufacturer's declaration. Static characteristics were experimentally recorded and are shown here. Figure 2 shows the dependence of the anode current from the anode voltage at the constant grid voltage ($V_g = 0$ V), and in Figure 3, the curves of the anode current and the current of the grid voltage from the grid voltage are shown in the constant anode voltage ($V_a = 3000$ V).

An iterative process achieved a good fit of the measured and simulated static characteristics, which provided a reliable simulation of the DC mode of the whole system. Adopted factory data on parasitic capacitances were sufficiently fitted with the results of the measurement of transient processes.

According to the previously described facts, the model for a specific VT was obtained as the following PSpice code:

```

*Simulator PSpice
*Device type: Power triode
*Device model: U1 GU62A
SUBCKT U1 A G K
*
*Calculate contribution to cathode current
*
Eat at 0 VALUE = {0.501*ATAN(V(A,K)/30)}
Eme me 0 VALUE = {PWR(LIMIT{V(A,K),0,10000},1.5)/4500}
Emu mu 0 VALUE = {V(G,K)}
Egs gs 0 VALUE = {LIMIT{V(A,K) + V(mu)*18.6,0,1E6}}

```

```

Egs2 gs2 0 VALUE = {PWRS(V(gs),1.5)*25E-6}
Ecath cc 0 VALUE = {LIMIT{V(gs2),0,V(me)}}
*
*Calculate anode current
*
Ga A K VALUE = {V(cc)}
*
*Calculate grid current
*
Gg G K VALUE = {PWR(LIMIT{V(G,K) + 1,0,1E6},1.5)*(2-V(at))*452E-6}
*
*Capacitance:
*
Cgk G K 80p
Cga A G 60p
ENDS
    
```

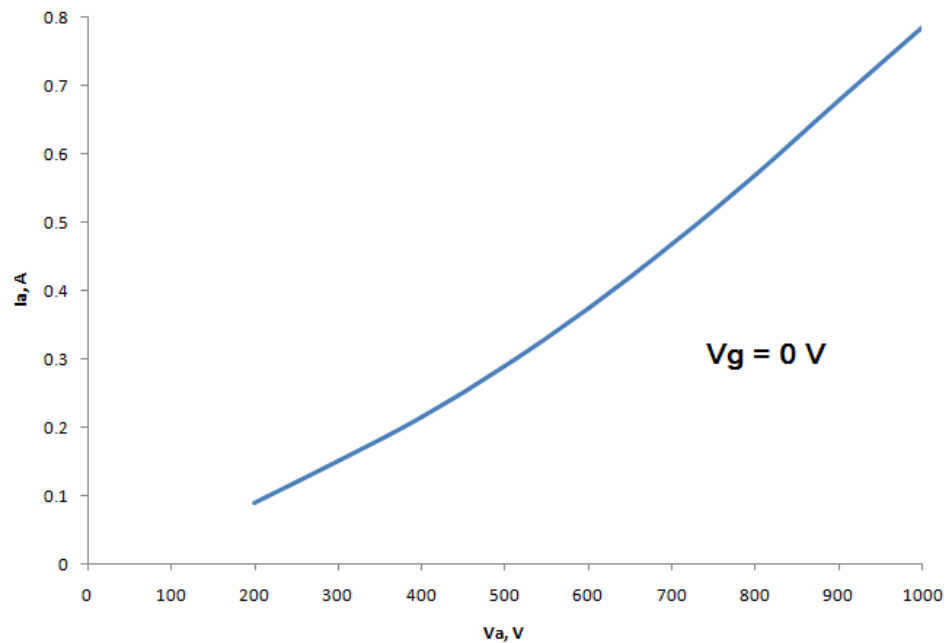


Figure 2. Chart of anodic current dependence on anode voltage at constant grid voltage.

The data in Table 3 describe the various components of the model and their interactions.

Table 3. The various components of the model and their interactions.

E_{at}	arctangent curve that is used to calculate the rise in grid current
E_{me}	cathode emission limit
E_{gs}	emission contribution from the grid and anode
E_{gs2}	E_{gs} after raising to the power of 3/2 and factored by a constant so that
E_{cath}	The cathode current value is the current between the anode and cathode
G_a	actual cathode current
G_g	grid current

The given VT model enables the completion of the electric circuit diagram for modelling and simulation of the designed HF generator. That PSpice model is shown in Figure 4.

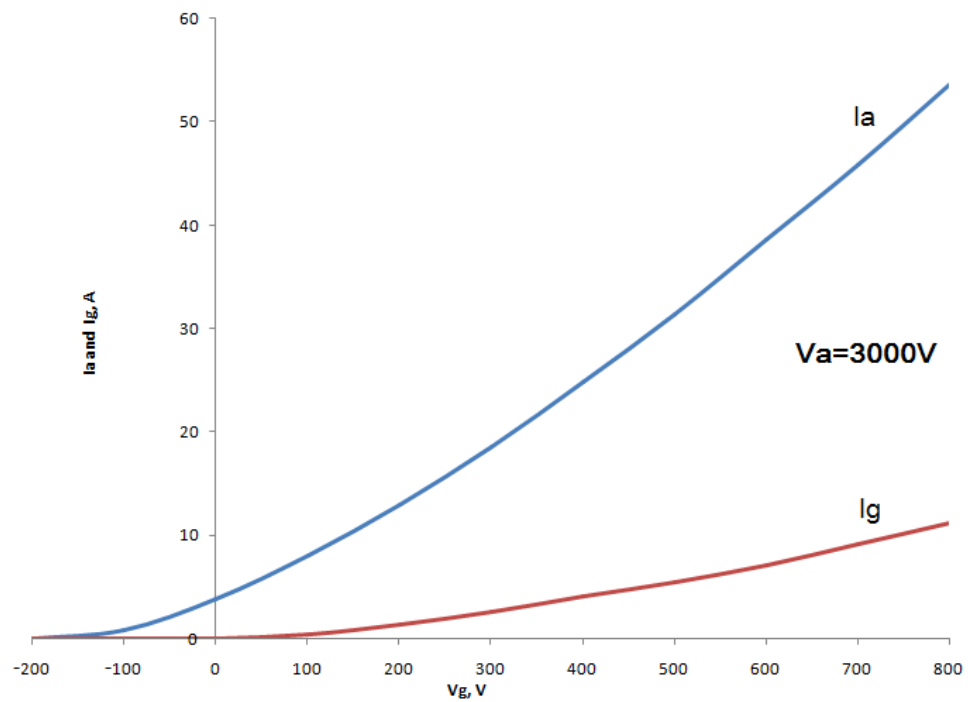


Figure 3. Graph of the dependence of anode current and grid current on grid voltage at constant anode voltage $V_a = 3000\text{ V}$.

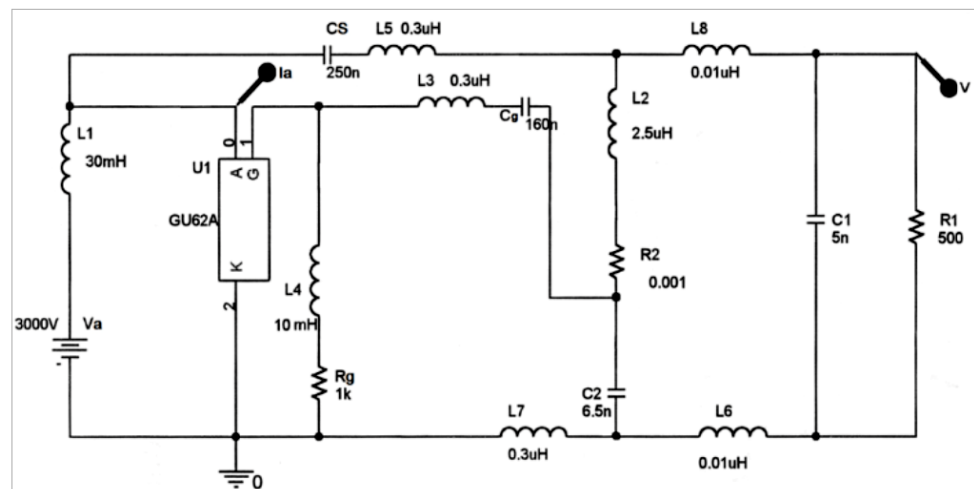


Figure 4. Complete circuit diagram for simulation of the designed generator.

Parasitic parameters were measured as much as possible and the final values were determined by an iterative process consisting of comparing the measurement and simulation results. In addition to the basic and parasitic elements, auxiliary elements R_g (resistor for VT grid pre-polarization) and L_4 (inductor for HF signals attenuation) are included in the scheme.

4. Computer Control

For signal generation and data acquisition, a measuring and control system based on the use of a personal computer (PC) was developed, which was schematically presented in Figure 5. In addition to PC, the hardware consisted of an AD/DA converter and external interface for analogue signals conditioning. AD/DA conversion was performed using a commercially available converter NI 6221 from National Instruments. National Instruments high-speed multifunction data acquisition (DAQ) devices were optimized for superior

accuracy at fast sampling rates. They had an onboard NI-PGIA2 amplifier designed for fast settling times and high scanning rates, ensuring 16-bit accuracy, even when measuring all channels at maximum speeds. All high speed devices had a minimum of 16 analogue inputs, 24 digital I/O lines, 7 programmable input ranges, analogue and digital triggering, and 2 counter/timers [31,32].

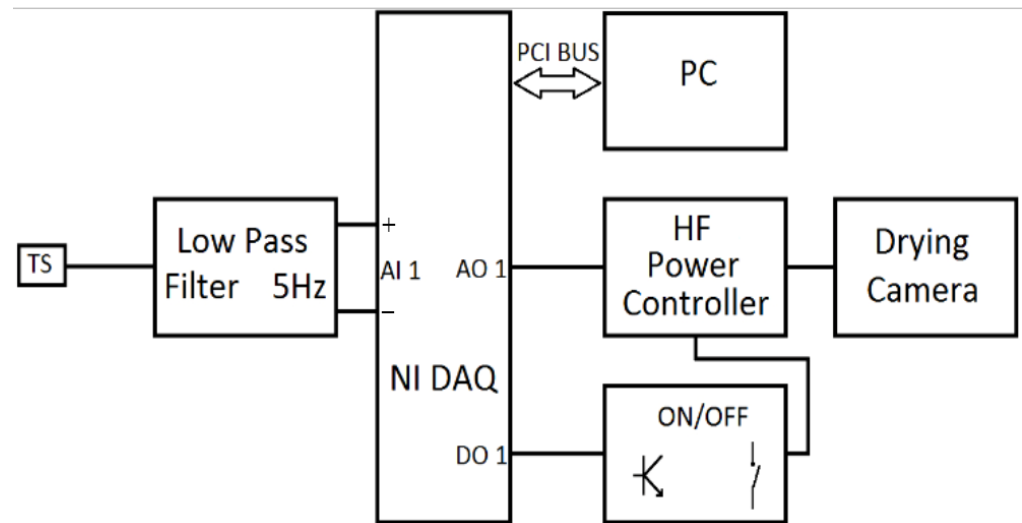


Figure 5. Block diagram of temperature regulation of wood drying system.

The software platform used for measurement methods was LabVIEW, which provided the reliable development of various modern virtual instruments. LabVIEW-based virtual instruments were implemented with the appropriate graphical user interface (GUI) [12]. GUI mainly consisted of two important components:

- control panel for process control and monitoring and
- application diagram, which presents used virtual instruments, relationships between them, the course of signals, and error detection.

In LabVIEW, a user interface was built by using a set of tools and objects. The user interface was known as the front panel. Then, the code was added using graphical representations of functions to control the front panel objects. The block diagram contained this code.

LabVIEW applications performed measurements, tests, and established process control, focusing on quick access to and view of the data. This software simplified hardware integration with the PC enabled quick collection and visualization of data sets from virtually any input/output device (I/O device). The advantage of using this development software was the reduced programming time, which was the result of a graphical program syntax that was more intuitive and did not require code writing. Using a graphic approach to programming, LabVIEW simplified complexly designed systems to simple graphics units that were intuitive and easy to use owing to an existence of variety of tools and appropriate documentation. LabVIEW-developed programs are called virtual instruments (VI) and they are recognizable by .vi filename extension [33–36].

The temperature control window is shown in Figure 6 and the corresponding application block diagram is presented in Figure 7.

DAQ Assistants were used for acquiring the input and generating output signals. The acquired signal from the temperature sensor was averaged because of eventual noise and measurement errors cancellation shown on the diagram, as well as saved in .txt file. Then, the PID controller calculated the current value of the output signal for the power controller based on the desired heating rate. Graphs, text inputs, text controls, and switches were also visible on the front panel, as well as access to the user for input parameters and viewing the final results.

Each conductive element is heated under the influence of the HF electric field, so the HF generator must be switched off periodically for 1 min in order to equalize the temperature of the sensor with the temperature of the wood. In order to reduce the heating of the sensor during normal operation of the HF generator, special Pt100 planar sensors with a thin film of platinum on a ceramic substrate were made. The plane of the sensor is placed parallel to the lines of the electric field, which minimizes the effect of the HF field.

A solution coded in this way in LabVIEW had a wider potential than the one highlighted here. Since all the results of LabVIEW program execution are recorded in the appropriate files, after a certain number of iterations, very usable data sets were obtained, which could be used as input based on real data for various calculations with the aim of improving understanding of the process and its components (for example, it could be used for predicting drying curves) [37]. Moreover, those data sets could further be reused and processed with new analyzes and syntheses using popular data science methods and methodologies (various predictive models, artificial neural networks, machine learning etc.) [38,39]. In this way, valuable insights could be obtained in a broader sense than the one presented in this paper, which suggested that the presented solution had its own sustainability and a wider field of application. Some new, hidden data could be discovered and further improvements made, both in this and in other areas of work. Furthermore, this trend is fully compatible with modern data management trends, which, among other things, highlights the reuse of obtained data. The multiple use of obtained data could provide various benefits in the form of saving resources, uncovering new knowledge, energy efficiency, etc. As can be seen from the above, the proposed solution can have a wider impact in various areas of its application and is not of a closed type, but can be further upgraded, improved, and adapted for different areas of application.

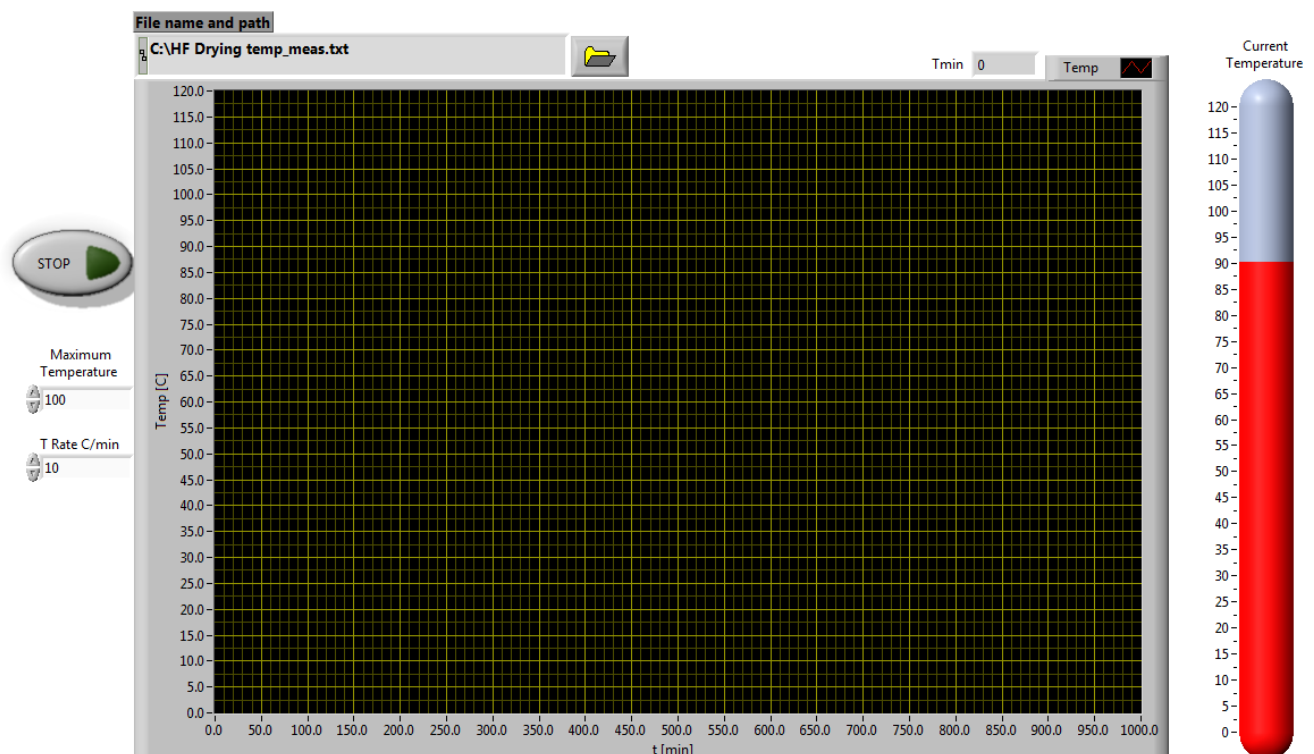


Figure 6. Temperature control front panel.

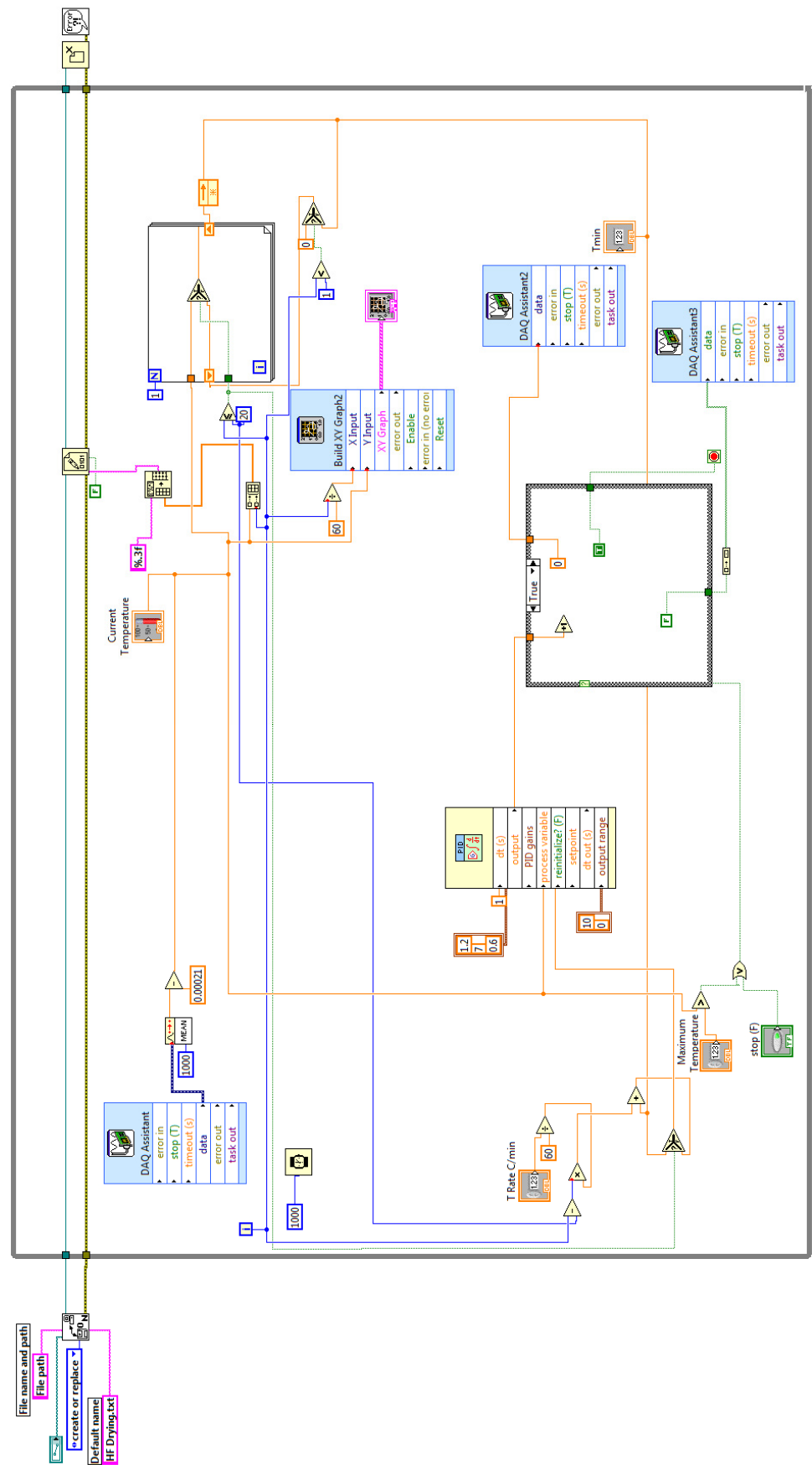


Figure 7. Application block diagram.

5. Simulation and Experimental Results

The described model was tested by comparing with the results of measurements on the real system, where the configuration of the wood complex, the humidity of the wood, and the frequencies were changed. After obtaining a high matching level of the simulation and measurement results, “experiments” were simulated on the simulator, in order to optimize the system parameters from the point of view of energy efficiency and other requirements.

The illustration in Figure 8 shows the simulated and measured consumer voltage values and the anode current for the designed generator with the values of real and parasitic elements as it is shown in Figure 4. For these conditions, the following values were measured:

1. Maximum value of anode voltage: $U_{ma} = 1930 \text{ V}$;
2. Anode current impulse intensity: $I_{ma} = 15.1 \text{ A}$;
3. Power consumption: $P_0 = 3.24 \text{ kW}$;
4. The power of anode dissociation: $P_a = 1.12 \text{ kW}$;
5. Active Consumer Power: $P = 2.12 \text{ kW}$;
6. Oscillation frequency: $f = 1.83 \text{ MHz}$.

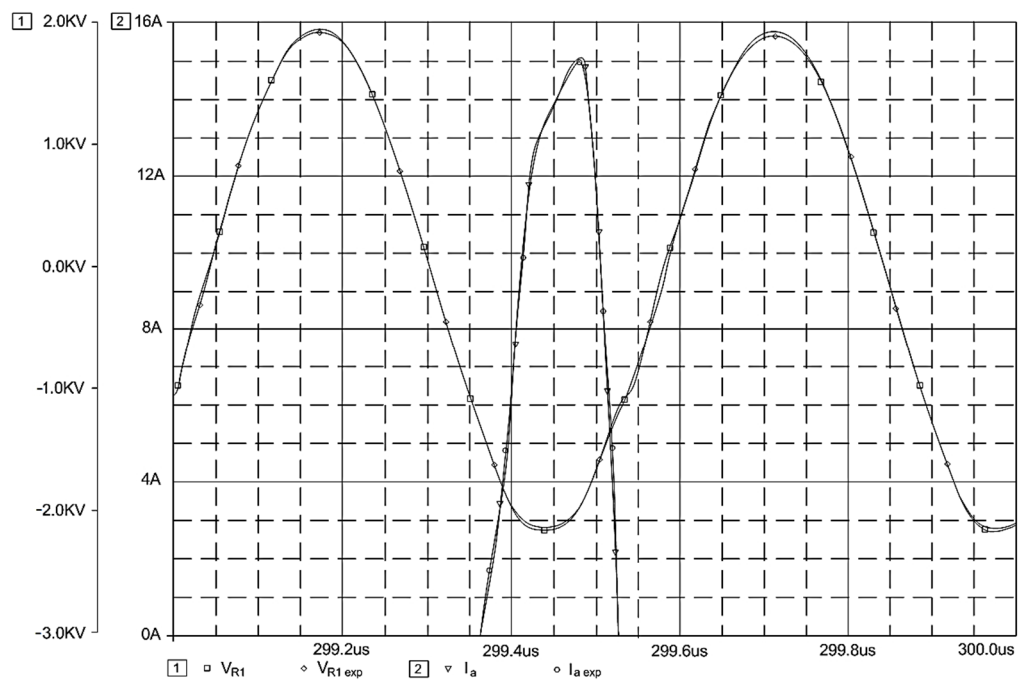


Figure 8. Results of the measurement and simulation for the consumer voltage and the anode current.

The obtained results greatly matched the simulation results, as well as the recommendations and parameters of the initial calculation; therefore, it can be concluded that the parameters, regime, and model adopted were well defined.

The results of measurement and simulation of the relevant electrical parameters of the HF generator in the given mode are given in Table 4.

Table 4. Measurement and simulation results.

Variable	Value
f	1.83 MHz
$V_{load \text{ exp}}$	1.54 kV
$V_{load \text{ sim}}$	1.63 kV
$I_a \text{ max exp}$	14.98 A
$I_a \text{ max sim}$	15.08 A

Variables shown in Table 4 represent the following:

f —operating frequency,

$V_{\text{load exp}}$ —measured effective value of the voltage on the load,

$V_{\text{load sim}}$ —the effective value of the voltage on the load obtained by simulation,

$I_{\text{a max exp}}$ —measured maximum value of anode current,

$I_{\text{a max sim}}$ —the maximum value of the anode current obtained by simulation.

6. Conclusions

An HF generator for wood drying based on VT was designed, modeled, and simulated. The first calculations were performed using a standard procedure, and then the parameters were optimized by modeling and simulation. The parameters of the selected VT triode model were adjusted based on the measured characteristics, and then the model was placed in the environment, taking into account the fundamental, auxiliary, and parasitic elements of the oscillator. A series of iterations were performed, with measurements in the real system, in order to adjust the model parameters and optimize the parameters. The experiments showed a high level of matching between simulation and measurement results. This confirmed the validity of the model and the possibility of further research in this scientific research area.

Additionally, the procedures presented in this paper enable the realization of some other benefits. Thanks to the described procedures, it was possible to adequately perform the simulation and obtain appropriate conclusions that could help to avoid oversizing the system, which could further produce unnecessary additional costs in the real implementations. Additionally, in future analyses and development of such and similar systems, thanks to the mentioned hardware-software components, it is possible to connect the traditional model-driven with a modern data-driven approach during various analyses and syntheses related to the various implementations of systems for drying wood. Finally, the existence of the proper simulations adds an educational component to the complete solution, since the simulations shown in this work can be used in a various education stages, for example in the education of future engineers of different profiles of technical professions (wood-processing, electrical engineering, mechanical engineering, etc.), but they can be used equally successfully in the education and training of end users, as well as of those who deal with the implementation and maintenance of the mentioned systems.

Author Contributions: Conceptualization, P.S. and Z.S.; methodology, P.S., Z.S., S.P. and V.N.; software, P.S., Z.S. and M.S.; validation, P.S., S.P., V.N. and D.K.; formal analysis, Z.S., S.P. and V.N.; investigation, P.S., Z.S. and M.S.; resources, P.S., Z.S. and M.S.; data curation, M.S.; writing—original draft preparation, P.S., Z.S. and V.N.; writing—review and editing, P.S. and Z.S.; visualization, S.P. and D.M.; supervision, P.S.; project administration, Z.S.; funding acquisition, Z.S. All authors have read and agreed to the published version of the manuscript.

Funding: This research was financially supported by the Ministry of Education, Science, and Technological Development of the Republic of Serbia, under contract number 451-03-68/2022-14.

Institutional Review Board Statement: Not applicable.

Informed Consent Statement: Not applicable.

Data Availability Statement: The data supporting reported results are included within the article.

Conflicts of Interest: The authors declare no conflict of interest. The funders had no role in the design of the study; in the collection, analyses, or interpretation of data; in the writing of the manuscript; or in the decision to publish the results.

Nomenclature

f	frequency of oscillation [Hz]
I	current [A]
L	inductance [H]
P	power [kW]
S	gradient of characteristics [mAV^{-1}]
U	voltage [V]
μ	amplification [/]

References

- Mali, S.B.; Butale, M.C. A Review Paper on Different Drying Methods. *Int. J. Eng. Res. Technol.* **2019**, *8*, 211–216.
- Rajewska, K.; Smoczkiwicz-Wojciechowska, A.; Majka, J. Intensification of beech wood drying process using microwaves. *Chem. Process Eng.* **2019**, *40*, 179–187.
- Klement, I.; Vilkovský, P.; Vilkovská, T. Change in Selected Mechanical Properties of Beech Wood at the Contact Drying. *Materials* **2022**, *15*, 7433. [[CrossRef](#)]
- Liu, H.; Zhang, J.; Jiang, W.; Cai, Y. Characteristics of Commercial-scale Radio-frequency/Vacuum (RF/V) Drying for Hardwood Lumber. *BioResources* **2019**, *14*, 6923–6935. [[CrossRef](#)]
- Dryakonov, K.F.; Goryaev, A.A. *Drying Wood by High Frequency Currents*; Wood Industry: Moscow, Russia, 1998.
- Rosebury, F. *Handbook of Electron Tube and Vacuum Techniques*; American Institute of Physics Melville: New York, NY, USA, 1993.
- Carter, R.G.R.F. Power Generation. In Proceedings of the CAS—CERN Accelerator School: RF for Accelerators, Ebeltoft, Denmark, 8–17 June 2010; CERN: Geneva, Switzerland, 2011; pp. 173–207.
- Clerc, G.; Ichac, J.P.; Robert, C. A new generation of gridded tubes for higher power and higher frequencies. In Proceedings of the 17th IEEE Particle Accelerator Conference (PAC 97): Accelerator Science, Technology and Applications, Vancouver, BC, Canada, 12–16 May 1997; JACoW Publishing: Geneva, Switzerland, 1997; pp. 2899–2901.
- Eichmeier, J.A.; Thumm, M. (Eds.) *Vacuum Electronics: Components and Devices*; Springer: Berlin, Germany, 2008.
- Whitaker, J. *Power Vacuum Tubes Handbook*; CRC Press: London, UK, 2017.
- Brounley, R.W. Mismatched Load Characterization for High-Power RF Amplifiers. *High Freq. Electron.* **2004**, *3*, 30–38.
- National Instruments. *LabVIEW Development Guidelines*; National Instruments Corporation: Austin, TX, USA, 2016.
- Vaščák, J.; Madarász, L. Automatic Adaptation of Fuzzy Controllers. *Acta Polytech. Hung.* **2005**, *2*, 5–18.
- Ma, M.; Zhang, Y.; Langholz, G.; Kandel, A. On direct construction of fuzzy systems. *Fuzzy Sets Syst.* **2000**, *112*, 165–171. [[CrossRef](#)]
- Tar, J.K.; Rudas, I.J.; Bitó, J.F. Comparison of the Operation of the Centralized and the Decentralized Variants of a Soft Computing Based Adaptive Control. In Proceedings of the Budapest Polytechnic Jubilee Conference: Science in Engineering, Economics and Education, Budapest, Hungary, 4 September 2004; pp. 331–342.
- Basciftci, F.; Hatay, O.F. Design of Saving Circuit with Fuzzy Logic Control for Residences and Small Scale Enterprises. *Adv. Electr. Comput. Eng.* **2010**, *10*, 99–102. [[CrossRef](#)]
- Lakhoua, M.N. Application of Functional Analysis on a SCADA System of a Thermal Power Plant. *Adv. Electr. Comput. Eng.* **2009**, *9*, 90–98. [[CrossRef](#)]
- Lyon, S.; Bowe, S.; Wiemann, M. *Understanding Vacuum Drying Technologies for Commercial Lumber—General Technical Report PPL-GTR-287*; U.S. Department of Agriculture, Forest Service, Forest Products Laboratory: Madison, WI, USA, 2021.
- Strata Energy Consulting and Efficient Energy International. *Direct Process Heating: Microwave and Radio Frequency—Technical Information Document 2019*; Energy Efficiency and Conservation Authority: Wellington, New Zealand, 2019.
- Stević, Z.; Nikolić, V.; Radovanović, I. High-frequency VT generator for wood drying system. In Proceedings of the 31th International Congress of Process Industry PROCESING '18, Bajina Basta, Serbia, 6–8 June 2018; Union of Mechanical and Electrotechnical Engineers and Technicians of Serbia (SMEITS)—Society for Process Engineering: Belgrade, Serbia, 2018; pp. 261–264.
- Murashov, I.; Zverev, S.; Smorodinov, V.; Grachev, S. Development of digital twin of high frequency generator with self-excitation in Simulink. *IOP Conf. Ser. Mater. Sci. Eng.* **2019**, *643*, 012078. [[CrossRef](#)]
- Li, H.; Liu, F. Wood Drying by High Frequency Discharge. In Proceedings of the 2012 Asia-Pacific Power and Energy Engineering Conference, Shanghai, China, 27–29 March 2012; IEEE: Piscataway, NJ, USA, 2012; pp. 1–3.
- Vania, M.W. *PRF-1150 13.56MHz 1kW Class E RF Generator: Doc #9200-0255, Rev 1*; Directed Energy, Inc.: Fort Collins, CO, USA, 2002.
- Albulet, M. *RF Power Amplifiers*; Noble Publishing Corporation: Atlanta, GA, USA, 2001.
- Agafonov, B.S. *Calculation of HF Generator Exploitation Regimes*; Radioelektronika: Moscow, Russia, 1997.
- Lobodzinskiy, V.A. *HF Generators Projecting*; Odessa Electrotechnical Institute: Odessa, Ukraine, 1983.
- Nabel, R. *PSpice User Manual*; Birzeit University/Electrical Engineering Department: Birzeit, West Bank, Palestine, 2010.
- Intusoft. *Personal Computer Circuit DesignTools, Model Libraries*; Intusoft: San Pedro, CA, USA, 1997.

29. Munro, D. PSpice Model SV811 Series. Available online: <http://www.duncanamps.com/pdf/sv811spicemod.pdf> (accessed on 19 October 2022).
30. Normann, P. *Design of Amplifiers in LTspice*; Uppsala University: Uppsala, Sweden, 2013.
31. National Instruments. *M Series User Manual*; National Instruments Corporation: Austin, TX, USA, 2016.
32. Zoran, S.; Stevic, M.; Rajčić-Vujasinović, M.; Mijailović, D. Computer controlled system for differential thermal analysis. In Proceedings of the XVIIth International scientific-practical conference Modern information and electronic technologies, Odessa, Ukraine, 23–27 May 2016; pp. 186–188.
33. Fuertes, J.J. A virtual laboratory of D.C. motors for learning control theory. *Int. J. Electr. Eng. Educ.* **2013**, *50*, 172–187. [[CrossRef](#)]
34. Abdulwahed, M.; Nagy, Z.K. The impact of different preparation modes on enhancing the undergraduate process control engineering laboratory: A comparative study. *Comput. Appl. Eng. Educ.* **2014**, *22*, 110–119. [[CrossRef](#)]
35. Popović, N.; Naumović, M.B. Virtual laboratory and learning management system in optimal control theory education. *Int. J. Electr. Eng. Educ.* **2016**, *53*, 1–14. [[CrossRef](#)]
36. Whitley, K.N.; Novick, L.R.; Fisher, D. Evidence in Favor of Visual Representation for the Dataflow Paradigm: An Experiment Testing LabVIEW's Comprehensibility. *Int. J. Hum.-Comput. Stud.* **2006**, *64*, 281–303. [[CrossRef](#)]
37. Simo-Tagne, M.; Ndi-Azese, M. Thermal, economic, and environmental analysis of a novel solar dryer for firewood in various temperate and tropical climates. *Sol. Energy* **2021**, *226*, 348–364. [[CrossRef](#)]
38. Chai, H.; Chen, X.; Cai, Y.; Zhao, J. Artificial Neural Network Modeling for Predicting Wood Moisture Content in High Frequency Vacuum Drying Process. *Forests* **2019**, *10*, 16. [[CrossRef](#)]
39. Yin, Q.; Liu, H.-H. Drying Stress and Strain of Wood: A Review. *Appl. Sci.* **2021**, *11*, 5023. [[CrossRef](#)]

Disclaimer/Publisher's Note: The statements, opinions and data contained in all publications are solely those of the individual author(s) and contributor(s) and not of MDPI and/or the editor(s). MDPI and/or the editor(s) disclaim responsibility for any injury to people or property resulting from any ideas, methods, instructions or products referred to in the content.